# Exciton energy transfer between the inner and outer tubes in double-walled carbon nanotubes

Hideki Hirori,[1,2] Kazunari Matsuda,[1,*] and Yoshihiko Kanemitsu[1,3,†]
[1]*Institute for Chemical Research, Kyoto University, Uji, Kyoto 611-0011, Japan*
[2]*Institute for Integrated Cell-Material Sciences, Kyoto University, Sakyo-ku, Kyoto 606-8501, Japan*
[3]*Photonics and Electronics Science and Engineering Center, Kyoto University, Kyoto 615-8510, Japan*
(Received 22 August 2008; published 24 September 2008)

We have studied photoluminescence (PL) spectrum and dynamics of the inner nanotubes in double-walled carbon nanotubes (DWNTs) and compared PL properties between DWNTs and single-walled carbon nanotubes (SWNTs). The PL peak energies of the inner tubes are redshifted from those of SWNTs with the same chiral indices. This PL redshift is enhanced with an increase in the inner tube diameter. The PL lifetime of DWNTs increases with a decrease in the inner tube diameter. The diameter dependence of PL dynamics is explained by exciton energy transfer between the inner and outer tubes through Förster-type dipole-dipole interaction.

DOI: 10.1103/PhysRevB.78.113409 PACS number(s): 73.63.Fg, 73.22.−f, 78.47.Cd, 78.67.Ch

Carbon nanotubes have been studied extensively over the past decade, both due to their fundamental physics interest and their potential applications in electronic and photonics devices.[1,2] Since the discovery of efficient photoluminescence (PL) from micelle-wrapped single-walled carbon nanotubes (SWNTs),[3] the optical properties of SWNTs have also attracted considerable attention. PL processes of carbon nanotubes are determined by the dynamics of stable excitons through enhanced Coulomb interactions in one-dimensional systems.[4–9] Essential information on exciton dynamics in carbon nanotubes has been provided by PL spectroscopy and transient absorption studies,[10–16] and it has been shown that the exciton dynamics in SWNTs are determined by radiative and nonradiative relaxation processes within the nanotubes and exciton energy transfer between tubes in the bundled nanotubes.[17–21]

Double-walled carbon nanotubes (DWNTs) are one of the excellent samples for studying exciton energy transfer because the inner tubes are isolated into an unperturbed environment by their surrounding outer tubes. Raman-scattering experiments have shown that inner tubes of DWNTs exhibit unusual narrow lines of the radial breathing mode.[22,23] This unperturbed environment allows examination of the intrinsic nature of the interwall interaction between the inner and outer tubes of DWNTs. Static PL spectroscopy study of peapod-derived DWNTs has indicated that a decrease in interwall distance causes PL quenching.[24] In contrast, the transient and static PL of the inner tubes of DWNTs showed distinct PL peaks with various chiral indices.[25] However, the mechanisms of the electronic interaction and the exciton energy transfer between the inner and outer tubes of DWNTs are not yet clear.

In this Brief Report, we have studied PL spectra and dynamics of the inner tubes of DWNTs. We found that the PL peaks of the inner tubes in DWNTs are redshifted from those of SWNTs with the same chiral indices and that this redshift is enhanced with increasing inner tube diameter. In addition, PL lifetimes of the inner tubes decrease with increasing inner tube diameter. The difference in PL spectrum and dynamics between DWNTs and SWNTs is caused by the screening effect due to the outer tubes and the exciton energy transfer between the inner and outer tubes.

DWNTs and SWNTs grown by HiPCO (Carbon Nanotechnology Inc.) were prepared in dispersion in $D_2O$ solutions with 0.5 wt % sodium dodecylbenzene sulfonate (SDBS), vigorously sonicated, and then centrifuged at 30 000 g for 5 h.[3] Transmission electron microscopy (TEM) analyses confirmed that the samples in this study consisted of DWNTs (~65%), with a small admixture of residual multiwalled carbon nanotubes (~30%) and SWNTs (<5%). The average interwall distance between the inner and outer tubes in DWNTs was about 0.4 nm.

Time-resolved PL measurements were performed by using femtosecond excitation correlation (FEC) spectroscopy.[15,26] Both DWNT and SWNT samples were excited with optical pulses from a Ti:sapphire laser with a central wavelength of 730 nm (1.70 eV), repetition rate of 80 MHz, ~100 fs pulse duration, and a spectral width of 8 nm. The two beams separated by the delay time were chopped at 1000 and 800 Hz and collinearly focused onto the same spot (~10 $\mu$m) on the samples at normal incidence. Using a photomultiplier tube and a lock-in amplifier, only the PL signal components modulated at the sum frequency (1800 Hz) were detected after the initial PL dispersion by a monochromator. The measurements were carried out under low excitation conditions (~10 $\mu J/cm^2$).

Figures 1(a) and 1(b) show the PL excitation (PLE) maps of the SWNTs and DWNTs, respectively. Each PL peak of the SWNTs comes from nanotubes with different chiral indices $(n,m)$. The chiral indices are determined according to the assignment scheme described in Refs. 27 and 28. Well-resolved PL signals of the DWNTs are observed in the PLE map. As the pattern in the PLE map of the DWNTs is similar to that of the SWNTs, the chiral indices $(n,m)$ in the DWNTs are assigned according to the same scheme for the SWNTs. As the amount of residual SWNTs (<5%) in the DWNT samples and the outer tubes showing PL in this energy region is sufficiently small to be excluded, the PL of DWNT samples is ascribed to the inner tubes.[25]

Figures 2(a) and 2(b) show the time-integrated PL spectra of the DWNTs and the SWNTs under continuous-wave excitation at room temperature by Ti:sapphire and He-Ne lasers (1.70 and 1.96 eV, respectively). The PL peaks of the DWNTs in the higher energy region are not shifted relative to those of the SWNTs, but those in the lower energy region are redshifted.

 

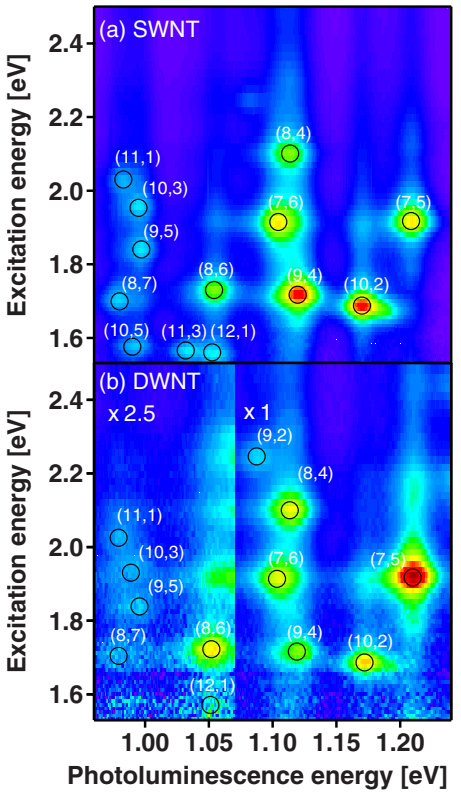


FIG. 1. (Color online) PL excitation maps of (a) SWNTs and (b) DWNTs. The assigned chiral indices are indicated in the figures.

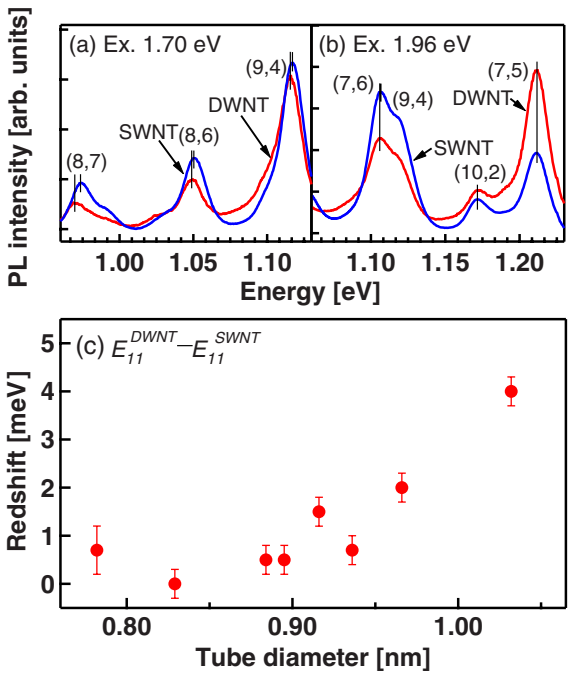


FIG. 2. (Color online) PL spectra of SWNTs and DWNTs under excitation at (a) 1.70 and (b) 1.96 eV. (c) Diameter dependence of the PL peak shift of DWNTs from the SWNTs with the same chiral indices.

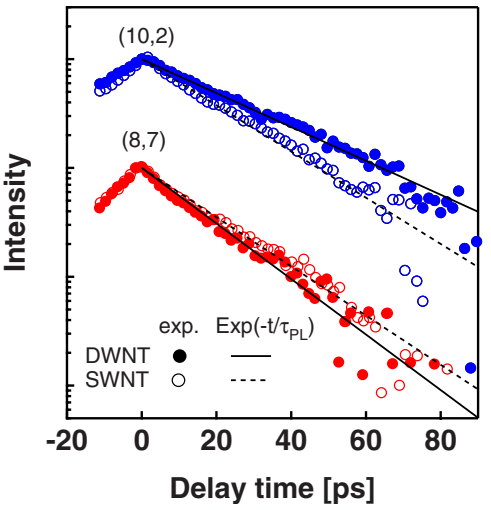


FIG. 3. (Color online) Normalized fast decay of the FEC signals of the DWNTs and SWNTs with different chiral indices: (10, 2) and (8, 7) measured under excitation at 1.70 eV. The solid (DWNTs) and dashed (SWNTs) lines represent the single exponential decay curves $\exp(-\tau/\tau_{PL})$. The upward direction on the vertical axis indicates that the FEC signals have negative sign.

Figure 2(c) shows the PL peak energy differences between $E_{11}^{DWNT}$ (DWNTs) and $E_{11}^{SWNT}$ (SWNTs) as a function of nanotube diameter. The PL peak redshift occurs in the DWNTs. The amount of redshift increases with inner tube diameter. External dielectric screening appears to be the dominant effect causing the PL peak redshift, since the electric-field lines between electrons and holes (excitons) experience sensitively the external dielectric constant $\varepsilon$. The change of exciton transition energy due to the dielectric screening is dominated by the band-gap shift rather than change of the exciton binding energy.[5,29] In fact, it has been reported that the PL peak energies of micelle-wrapped SWNTs in water or organic solvents ($\varepsilon \sim 2$) are redshifted away from those of SWNTs ($\sim$20–50 meV) suspended in air or vacuum ($\varepsilon \sim 1$).[30,31] The dielectric screening for inner tubes of DWNTs due to the outer tube ($\varepsilon \sim 4$) causes the PL redshift in DWNTs (Ref. 32) because of the small interwall distance in DWNTs ($\sim$0.4 nm). The diameter dependence of the PL redshift shown in Fig. 2(c) suggests that the dielectric screening is enhanced due to the shorter interwall distance between the inner and outer tubes with increasing inner tube diameter.

In order to clarify the effects of interwall distance on PL properties, we study the PL dynamics of DWNTs. Figure 3 shows the normalized fast-decay components of FEC signals.[15] In this picosecond time region, the decay curves are described by single exponential functions, and the PL lifetimes $\tau_{PL}$ are determined from the fast-decay component of FEC signal. In a smaller-diameter (10, 2) nanotube, the PL lifetime of DWNTs is larger than that of SWNTs. In a larger-diameter (8, 7) nanotube, the PL lifetime of DWNTs becomes shorter and close to that of SWNTs. Therefore, the PL dynamics depends on the diameter of the inner tube.

Figure 4 summarizes the PL lifetimes $\tau_{PL}$ as a function of tube diameter. The PL lifetime of DWNTs increases with

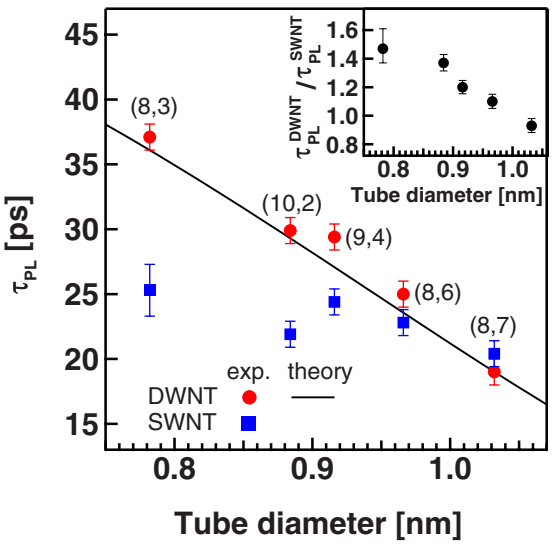


FIG. 4. (Color online) PL lifetimes $\tau_{PL}^{DWNT}$ and $\tau_{PL}^{SWNT}$ as a function of tube diameter in the DWNTs and SWNTs are denoted by solid circles and squares, respectively. The solid line shows the theoretically calculated curve using Eq. (3). The inset shows the PL lifetime ratio of DWNTs to SWNTs $\tau_{PL}^{DWNT}/\tau_{PL}^{SWNT}$ as a function of the tube diameter.

decreasing inner tube diameter, while the lifetime of SWNTs is almost independent of tube diameter. The inset of Fig. 4 shows the PL lifetime ratio of DWNTs to SWNTs $\tau_{PL}^{DWNT}/\tau_{PL}^{SWNT}$ as a function of tube diameter. The large diameter dependence of the PL lifetime ratio clearly indicates the existence of a fast energy relaxation process in DWNTs. As discussed in Fig. 2, the interwall distance is thought to become shorter for DWNTs with larger inner tubes. Therefore, we discuss the PL lifetime of DWNTs as a function of interwall distance.

First, we consider that the radiative lifetime decreases because of the enhancement of the dielectric screening effect in the larger inner tube, as discussed in the origin of the PL peak energy shift [see, Fig. 2(c)]. We estimate the decrease of the effective radiative lifetime when the effective dielectric constant $\varepsilon_{eff}$ increases. The increase of the effective dielectric constant of (8, 7) inner tube in comparison with (8, 7) SWNT is estimated as ~10% from the PL redshift of ~4 meV in Fig. 2(c).[33] The effective radiative lifetime is determined by both the radiative lifetime of the bright exciton state and the energy splitting between the bright and dark exciton states.[6,7,34] These two values depend on $\varepsilon_{eff}$. The change of the radiative lifetime of the bright exciton is estimated as only ~10% from Ref. 7, when $\varepsilon_{eff}$ increases about 10%. The change of the exciton splitting energy does not play an essential role in the decrease of the PL lifetime because at room temperature the thermal energy is much larger than the exciton splitting energy.[35] Hence, it is believed that the decrease of the PL lifetime in the larger inner tube cannot be explained only by the enhancement of the dielectric screening effect.

Next, we consider that the dependence of the PL lifetime on the interwall distance is caused by the exciton energy transfer from the inner (donor) to the outer (acceptor) tubes via Förster-type dipole-dipole interaction.[17,18] The energy-transfer efficiency is then determined by the interwall distance and the spectral overlap of donor emission and acceptor absorption.[36] For DWNTs, the emission spectra of excitonic states $E_{11}$ of inner tubes could overlap with the $E_{22}$ absorption spectra of outer tubes.

Using Förster's formalism, the total-energy transfer rate $1/\tau_{ET}$ can be described by integrating the rate over the entire surface of the outer tube as follows:[18,37]

$$\frac{1}{\tau_{ET}} = \frac{1}{\tau_{r,inner}^{DWNT}} \int_{-\infty}^{\infty} \int_{0}^{2\pi} \frac{d_{out}}{2} \left( \frac{R_0}{R(\theta,z)} \right)^6 dz d\theta$$

$$= \frac{1}{\tau_{r,inner}^{DWNT}} \int_{-\infty}^{\infty} \int_{0}^{2\pi} \frac{d_{out}}{2} \times \left( \frac{R_0}{\sqrt{(d_{in}/2)^2 + (d_{out}/2)^2 - d_{in} d_{out} \cos\theta/2 + z^2}} \right)^6 dz d\theta, \quad (1)$$

where $\tau_{r,inner}^{DWNT}$ is the radiative lifetime of the inner tube, $R_0$ is the Förster radius, $d_{in}$ is the inner tube diameter, and $d_{out}$ is the average diameter of the outer tube (~1.8 nm as determined from TEM measurements). As the observed PL lifetimes of SWNTs and DWNTs (~20–40 ps) are much shorter than the theoretically predicted radiative lifetime of the excitons in the SWNTs,[6,7] thus, the experimentally observed PL lifetime of the inner tube of DWNTs is determined by the nonradiative recombination $\tau_{nr,inner}^{DWNT}$ and exciton energy-transfer time $\tau_{ET}$:

$$(\tau_{PL,inner}^{DWNT})^{-1} \approx (\tau_{nr,inner}^{DWNT})^{-1} + (\tau_{ET})^{-1}. \quad (2)$$

Using Eqs. (1) and (2), the PL lifetime $\tau_{PL,innr}^{DWNT}$ can be derived as

$$\tau_{PL,inner}^{DWNT} \approx \tau_{nr,inner}^{DWNT} \left[ 1 + \frac{3\pi}{16} Q \frac{d_{out} R_0^6}{d^5} \int_0^{2\pi} \times \left( 1 - \frac{d_{in} d_{out}}{2d^2} \cos\theta \right)^{-5/2} d\theta \right]^{-1}, \quad (3)$$

where $d = \sqrt{(d_{in}/2)^2 + (d_{out}/2)^2}$. Assuming that the quantum yields of the inner tubes without exciton energy transfer $Q \approx \tau_{nr,inner}^{DWNT}/\tau_{r,inner}^{DWNT}$ is of the order of $10^{-3}$ similar to SWNTs,[10] we obtained the fitting curve shown in Fig. 4. We derived the best fitting parameters $\tau_{nr,inner}^{DWNT}$ of ~80 ps and the Förster radius of ~1.8 nm. The larger $\tau_{nr,inner}^{DWNT}$ (~80 ps) without energy transfer in comparison with PL lifetimes of SWNTs $\tau_{PL}^{SWNT} \approx \tau_{nr}^{SWNT}$ (~20 ps) implies that the inner tubes are clean and well shielded from the surrounding environments by the outer tube and preclude chemical derivatizations and defects on the sidewall, which could induce additional nonradiative relaxation paths.[38] Förster's theory predicted that energy could be transferred by a resonance dipole-dipole interaction mechanism over distances from ~1 to ~10 nm,[36] and thus the Förster radius of ~1.8 nm obtained here is reasonable. The diameter dependence of the observed $\tau_{PL,inner}^{DWNT}$ is well reproduced by the theory considering only Förster-type interaction. These results represent the evidence

that efficient exciton energy transfer occurs from inner to outer tubes in DWNTs.

In conclusion, we have studied PL spectra and dynamics in DWNTs to elucidate the mechanism of interactions between the inner and outer tubes. The PL peaks of the large inner tubes of the DWNTs are shifted to lower energies than those of SWNTs. The exciton energies of the inner tubes are affected by the outer tubes in the DWNTs. Furthermore, with an increase in inner tube diameter, the PL lifetimes of the inner tubes decrease. This diameter dependence suggests that exciton energy transfer occurs from the inner to the outer tubes in DWNTs and that the exciton energy transfer is caused by Förster-type dipole-dipole interaction. Our results indicate that exciton energy transfer, as well as electronic screening, plays a crucial role in interwall interactions of DWNTs.

The authors would like to thank Y. Watanabe for the PL map measurements. Part of this work was supported by the MEXT Joint Project of Chemical Synthesis Core Research Institutions and the Grant-in-Aid for Scientific Research from JSPS (Contracts No. 20048004 and No. 20340075).

*matsuda@scl.kyoto-u.ac.jp
†kanemitu@scl.kyoto-u.ac.jp

[1] R. Saito, G. Dresselhaus, and M. S. Dresselhaus, *Physical Properties of Carbon Nanotubes* (Imperial College Press, London, 1998).
[2] Ph. Avouris, M. Freitag, and V. Perebeinos, Nat. Phys. **2**, 341 (2008).
[3] M. J. O'Connell, S. M. Bachilo, C. B. Huffman, V. C. Moore, M. S. Strano, E. H. Haroz, K. L. Rialon, P. J. Boul, W. H. Noon, C. Kittrell, J. Ma, R. H. Hauge, R. B. Weisman, and R. E. Smalley, Science **297**, 593 (2002).
[4] T. Ogawa and T. Takagahara, Phys. Rev. B **43**, 14325 (1991).
[5] T. Ando, J. Phys. Soc. Jpn. **66**, 1066 (1997).
[6] C. D. Spataru, S. Ismail-Beigi, R. B. Capaz, and S. G. Louie, Phys. Rev. Lett. **95**, 247402 (2005).
[7] V. Perebeinos, J. Tersoff, and Ph. Avouris, Nano Lett. **5**, 2495 (2005).
[8] F. Wang, G. Dukovic, L. E. Brus, and T. F. Heinz, Science **308**, 838 (2005).
[9] J. Maultzsch, R. Pomraenke, S. Reich, E. Chang, D. Prezzi, A. Ruini, E. Molinari, M. S. Strano, C. Thomsen, and C. Lienau, Phys. Rev. B **72**, 241402(R) (2005).
[10] F. Wang, G. Dukovic, L. E. Brus, and T. F. Heinz, Phys. Rev. Lett. **92**, 177401 (2004).
[11] G. N. Ostojic, S. Zaric, J. Kono, M. S. Strano, V. C. Moore, R. H. Hauge, and R. E. Smalley, Phys. Rev. Lett. **92**, 117402 (2004).
[12] O. J. Korovyanko, C.-X. Sheng, Z. V. Vardeny, A. B. Dalton, and R. H. Baughman, Phys. Rev. Lett. **92**, 017403 (2004).
[13] S. Reich, M. Dworzak, A. Hoffmann, C. Thomsen, and M. S. Strano, Phys. Rev. B **71**, 033402 (2005).
[14] A. Hagen, M. Steiner, M. B. Raschke, C. Lienau, T. Hertel, H. Qian, A. J. Meixner, and A. Hartschuh, Phys. Rev. Lett. **95**, 197401 (2005).
[15] H. Hirori, K. Matsuda, Y. Miyauchi, S. Maruyama, and Y. Kanemitsu, Phys. Rev. Lett. **97**, 257401 (2006).
[16] S. Berger, C. Voisin, G. Cassabois, C. Delalande, and P. Roussignol, Nano Lett. **7**, 398 (2007).
[17] P. H. Tan, A. G. Rozhin, T. Hasan, P. Hu, V. Scardaci, W. I. Milne, and A. C. Ferrari, Phys. Rev. Lett. **99**, 137402 (2007).
[18] H. Qian, C. Georgi, N. Anderson, A. A. Green, M. C. Hersam, L. Novotny, and A. Hartschuh, Nano Lett. **8**, 1363 (2008).
[19] O. N. Torrens, D. E. Milkie, M. Zheng, and J. M. Kikkawa, Nano Lett. **6**, 2864 (2006).
[20] K. Matsuda, T. Inoue, Y. Murakami, S. Maruyama, and Y. Kanemitsu, Phys. Rev. B **77**, 193405 (2008).
[21] B. F. Habenicht and O. V. Prezhdo, Phys. Rev. Lett. **100**, 197402 (2008).
[22] R. Pfeiffer, H. Kuzmany, Ch. Kramberger, Ch. Schaman, T. Pichler, H. Kataura, Y. Achiba, J. Kürti, and V. Zólyomi, Phys. Rev. Lett. **90**, 225501 (2003).
[23] R. Pfeiffer, F. Simon, H. Kuzmany, and V. N. Popov, Phys. Rev. B **72**, 161404(R) (2005).
[24] T. Okazaki, S. Bandow, G. Tamura, Y. Fujita, K. Iakoubovskii, S. Kazaoui, N. Minami, T. Saito, K. Suenaga, and S. Iijima, Phys. Rev. B **74**, 153404 (2006).
[25] T. Hertel, A. Hagen, V. Talalaev, K. Arnold, F. Hennrich, M. Kappes, S. Rosenthal, J. McBride, H. Ulbricht, and E. Flahaut, Nano Lett. **5**, 511 (2005).
[26] D. von der Linde, J. Kuhl, and E. Rosengart, J. Lumin. **24–25**, 675 (1981).
[27] S. M. Bachilo, M. S. Strano, C. Kittrell, R. H. Hauge, R. E. Smalley, and R. B. Weisman, Science **298**, 2361 (2002).
[28] R. B. Weisman and S. M. Bachilo, Nano Lett. **3**, 1235 (2003).
[29] T. Ogawa and T. Takagahara, Phys. Rev. B **44**, 8138 (1991).
[30] Y. Ohno, S. Iwasaki, Y. Murakami, S. Kishimoto, S. Maruyama, and T. Mizutani, Phys. Rev. B **73**, 235427 (2006).
[31] O. Kiowski, S. Lebedkin, F. Hennrich, S. Malik, H. Rösner, K. Arnold, C. Sürgers, and M. M. Kappes, Phys. Rev. B **75**, 075421 (2007).
[32] T. G. Pedersen, Phys. Rev. B **67**, 113106 (2003).
[33] Y. Miyauchi, R. Saito, K. Sato, Y. Ohno, S. Iwasaki, T. Mizutani, J. Jiang, and S. Maruyama, Chem. Phys. Lett. **442**, 394 (2007).
[34] V. Perebeinos, J. Tersoff, and Ph. Avouris, Phys. Rev. Lett. **92**, 257402 (2004).
[35] I. B. Mortimer and R. J. Nicholas, Phys. Rev. Lett. **98**, 027404 (2007); R. Matsunaga, K. Matsuda, and Y. Kanemitsu, *ibid.* (to be published).
[36] R. M. Clegg, in *Fluorescence Imaging Spectroscopy and Microscopy*, edited by X. F. Wang and B. Herman (Willey, New York, 1996), Chap. 7.
[37] Here, we assume that a cross section of a nanotube is on $x$-$y$ plane and the length of nanotube is along the $z$ axis. The $R$ is defined by the distance between the fixed point on the inner tube and the certain point on the outer tube ($p_{\mathrm{out}}$). The line between $p_{\mathrm{out}}$ and the center of the nanotube makes an angle $\theta$ with $x$ axis. Thus, $R$ is represented by $R(\theta,z) = \sqrt{(d_{\mathrm{in}}/2)^2+(d_{\mathrm{out}}/2)^2-d_{\mathrm{in}}d_{\mathrm{out}}\cos\theta/2+z^2}$ as a function of $\theta$ and $z$.
[38] L. Cognet, D. A. Tsyboulski, J.-D. R. Rocha, C. D. Doyle, J. M. Tour, and R. B. Weisman, Science **316**, 1465 (2007).